bioRxiv preprint doi: https://doi.org/10.1101/2024.06.02.597063; this version posted June 3, 2024. The copyright holder for this preprint (which was not certified by peer review) is the author/funder, who has granted bioRxiv a license to display the preprint in perpetuity. It is made available under a CC-BY-NC-ND 4.0 International license.

Effects of Tasks on Functional Brain Connectivity Derived from Inter-Individual Correlations: Insights from Regional Homogeneity of Functional MRI Data

Xin Di [1*], Pratik Jain [1], Bharat B. Biswal [1*]

1. Department of Biomedical Engineering, New Jersey Institute of Technology, Newark, NJ, 07102, USA

* Corresponding author:

Xin Di, Ph.D.

604 Fenster Hall, University Height

Newark, NJ, 07102, USA

xin.di@njit.edu

Bharat B. Biswal, Ph.D.

607 Fenster Hall, University Height

Newark, NJ, 07102, USA

bbiswal@yahoo.com

bioRxiv preprint doi: https://doi.org/10.1101/2024.06.02.597063; this version posted June 3, 2024. The copyright holder for this preprint (which was not certified by peer review) is the author/funder, who has granted bioRxiv a license to display the preprint in perpetuity. It is made available under a CC-BY-NC-ND 4.0 International license.

Abstract

Research on brain functional connectivity often relies on intra-individual moment-to-moment correlations of functional brain activity, typically using techniques like functional MRI (fMRI). Inter-individual correlations are also employed on data from fMRI and positron emission tomography (PET). Many past studies have not specified tasks for participants, keeping them in an implicit "resting" condition. This lack of task specificity raises questions about how different tasks impact inter-individual correlation estimates. In our analysis of fMRI data from 100 unrelated participants, scanned during seven task conditions and in a resting state, we calculated Regional Homogeneity (ReHo) for each task as a regional measure of brain functions. We found that changes in ReHo due to different tasks were relatively small compared with the variations across brain regions. Cross-region variations of ReHo were highly correlated between different tasks. Similarly, whole-brain inter-individual correlation patterns were remarkably consistent across the tasks, showing correlations greater than 0.78. Changes in inter-individual correlations between tasks were primarily driven by connectivity in the visual, somatomotor, default mode network, and the interactions between them. The subtle yet statistically significant differences in functional connectivity may be linked to specific brain regions associated with the studied tasks. Future studies should consider task design when exploring inter-individual connectivity in specific brain systems.

Keywords: Brain connectivity, covariance network, molecular connectivity, motor network, task modulation.

bioRxiv preprint doi: https://doi.org/10.1101/2024.06.02.597063; this version posted June 3, 2024. The copyright holder for this preprint (which was not certified by peer review) is the author/funder, who has granted bioRxiv a license to display the preprint in perpetuity. It is made available under a CC-BY-NC-ND 4.0 International license.

1. Introduction

An important goal of brain research is to understand the brain connectivity between remote brain regions (Friston, 2011, 1994). Functional connectivity is mainly studied based on moment-to-moment correlations of brain measures from functional MRI (fMRI) (Biswal et al., 1995, 2010; Fox et al., 2005). An alternative approach is to estimate functional connectivity based on inter-individual correlations of brain functional measures, such as glucose metabolic activity measured using [^{18}F]fluorodeoxyglucose ([^{18}F]FDG) positron emission tomography (PET) (Horwitz et al., 1984; Metter et al., 1984). Inter-individual covariance of functional structural brain measures have been used for characterizing brain connectivity in both fMRI (Taylor et al., 2012) and PET studies (Di et al., 2017a; Di and Biswal, and Alzheimer's Disease Neu, 2012).

Studies have shown that the inter-individual correlation approach can produce connectivity that are similar to those derived from moment-to-moment correlations using fMRI (Di et al., 2017a) and anatomical connectivity derived from diffusion weighted imaging (Lizarraga et al., 2023). More importantly, the inter-individual approach can take advantage of molecular imaging to measure different aspects of physiology related to neuronal activity (Sala et al., 2023). For example, molecular imaging using PET can measure cerebral blood flow with [^{15}O]H_2O (Frackowiak et al., 1980), glucose metabolism using (F-18)2-fluoro-2-deoxy-D-glucose (FDG) (Phelps et al., 1979), and others (Fang et al., 2021). For fMRI, different types of parameters can also be exploit to reveal different aspects of functions (Taylor et al., 2012). Therefore, although limited by the amount of data, the inter-individual approach could provide unique information regarding brain functional organizations.

Most previous studies do not ask the participants to perform a specific task or place the participants with an explicit "resting" condition. It remains unclear how different task conditions may affect the estimates of functional covariance measures of functional connectivity. Studies using PET have shown that regional functional measures of cerebral blood flow and glucose metabolism were modulated by task conditions in a regionally selective manner. That is, there are certain sets of regions that involved in a particular task performance showed differences in the tasks. These task-specific regional signals may

bioRxiv preprint doi: https://doi.org/10.1101/2024.06.02.597063; this version posted June 3, 2024. The copyright holder for this preprint (which was not certified by peer review) is the author/funder, who has granted bioRxiv a license to display the preprint in perpetuity. It is made available under a CC-BY-NC-ND 4.0 International license.

enhance or at least modulate inter-individual correlations between the given region and other brain regions. Alternatively, the enhanced activity might reduce the inter-individual variability, therefore reducing connectivity estimates. In any circumstance, task may lead to changes in inter-individual correlations. However, studies on within individual measures of functional connectivity generally showed that functional connectivity was largely similar across tasks (Cole et al., 2014; Di et al., 2020), and changes in connectivity between task conditions are rather small compared with their absolute values (Cole et al., 2014; Di and Biswal, 2019). The question becomes to what extend is inter-individual connectivity modulated by different task conditions.

Collecting PET data for multiple tasks from the same individuals presents challenges, while obtaining fMRI data, especially when large-scale datasets like the Human Connectome Project (HCP) (Barch et al., 2013) are available, is relatively straightforward. In the HCP dataset, for instance, participants underwent MRI scanning while performing various tasks. We measured functional activations during different tasks using the HCP dataset by using regional homogeneity (ReHo) (Zang et al., 2004), which summarizes brain activations over a period, usually a few minutes. ReHo has demonstrated correlations \with PET and fMRI measures of cerebral blood flow and glucose metabolism (Adhikari et al., 2022; Aiello et al., 2015; Li et al., 2012; Wang et al., 2021). It has also been utilized to derive resting-state functional brain networks using resting-state data (Taylor et al., 2012). In the current study, we further ask how functional connectivity derived from cross-subject correlations of ReHo was modulated by different task conditions.

We first hypothesize that ReHo is a valid measure of brain functions, therefore could show regional alterations in different task conditions according to the task demands. We predict that alteration in ReHo in a task may involve regions that associated with certain task components. We are particularly interested in the extent of changes in ReHo due to task conditions, compared with the variations across different brain regions. Next, we hypothesize that inter-individual correlations of ReHo would be similar across different task conditions. However, we are still interested in specific connections that showed variable connectivity in different task conditions.

bioRxiv preprint doi: https://doi.org/10.1101/2024.06.02.597063; this version posted June 3, 2024. The copyright holder for this preprint (which was not certified by peer review) is the author/funder, who has granted bioRxiv a license to display the preprint in perpetuity. It is made available under a CC-BY-NC-ND 4.0 International license.

2. Methods

2.1. MRI data and task design

We conducted an analysis of fMRI data from 100 unrelated participants from the Human Connectome Project (HCP) (Barch et al., 2013), encompassing resting-state scans and seven tasks. Among these participants, 54 were females. Their ages were provided in ranges rather than specific years: 22-25 years (17 participants), 26-30 years (40 participants), 31-35 years (42 participants), and older than 36 years (1 participant).

The participants engaged in seven tasks and a resting state during MRI scanning. These tasks were structured as block designs, each comprising one or more task conditions, corresponding control conditions, and a fixation condition. The resting state is a special task, where participants were instructed to keep their eyes open, avoid falling asleep, and think of nothing in particular. They viewed a "relaxed" fixation, represented by a white cross on a dark background (Smith et al., 2013). With the exception of the language task, which involved auditory stimuli, all tasks utilized visual stimuli or instructions. In each task, participants were required to respond after receiving stimuli, while no response was needed during the resting-state condition. Table 1 provides a breakdown of task parameters for each task.

Task	# of images	# of runs	Stimuli modality	Response
Emotion	176	2	Visual	Yes
Gambling	253	2	Visual	Yes
Language	316	2	Auditory	Yes
Motor	284	2	Visual	Yes
Relational	232	2	Visual	Yes
Social	274	2	Visual	Yes
Working memory	405	2	Visual	Yes
Resting state	1,200	4	Visual	No

Table 1 Imaging and task design information for different task conditions.

We used the minimally preprocessed data in the current analysis. The MRI data were acquired using Siemens' standard 32-channel head coil. Each task underwent two fMRI runs, with variable

bioRxiv preprint doi: https://doi.org/10.1101/2024.06.02.597063; this version posted June 3, 2024. The copyright holder for this preprint (which was not certified by peer review) is the author/funder, who has granted bioRxiv a license to display the preprint in perpetuity. It is made available under a CC-BY-NC-ND 4.0 International license.

durations for different tasks. For each task, one run utilized right-to-left phase encoding, while the other run employed left-to-right phase encoding. While the resting-state task were scanned four runs, with twice in each phase encoding. The fMRI scanning parameters were as follows: repetition time (TR) = 720 ms; echo time (TE) = 33.1 ms; flip angle (FA) = 52°; field of view (FOV) = 208 × 180 mm²; slice number = 72; voxel size = 2.0 mm isotropic; multiband factor = 8. The T1-weighted MRI scanning parameters were: TR = 2400 ms; TE = 2.14 ms; FA = 8°; FOV = 224 × 224; voxel size = 0.7 isotropic.

2.2. Analysis software

The image processing and data analysis were performed in MATLAB (https://www.mathworks.com), with in-house codes and codes from statistical parametric mapping (SPM12; https://www.fil.ion.ucl.ac.uk/spm/) and Resting-State fMRI Data Analysis Toolkit v1.8 (Song et al., 2011). BrainNetViewer was used for visualization of brain regions and connections (Xia et al., 2013).

2.3. Calculation of ReHo

ReHo was computed as a regional functional measure for each task run (Taylor et al., 2012; Zang et al., 2004). An intracranial mask was created by combining the intracranial mask from SPM with available functional images for each participant. Furthermore, the mean ReHo value across all voxels within the intracranial mask was calculated as a global ReHo value, which will be used to standardize regional ReHo values later.

2.4. Regions of interest (ROIs)

We adopted Shaefer's 100-region parcellation for the cortex (Schaefer et al., 2018). In addition, subcortical regions were also included based on automated anatomical labeling atlas (Tzourio-Mazoyer et al., 2002). The 14 included subcortical nuclei were bilateral hippocampus, parahippocampus, amygdala, caudate, putamen, pallidum, and thalamus. For the Schaefer atlas, the regions were separated by the left (#1 to #50) and right (#51 to #100) hemispheres and were further divided into seven networks, including visual, sensorimotor, dorsal attention, salience/ventral attention, limbic, control, and default mode networks. In total, 114 regions of interest (ROIs) were used. For each task run, averaged ReHo values were extracted for each ROI, and were divided by the global ReHo value of the participant.

bioRxiv preprint doi: https://doi.org/10.1101/2024.06.02.597063; this version posted June 3, 2024. The copyright holder for this preprint (which was not certified by peer review) is the author/funder, who has granted bioRxiv a license to display the preprint in perpetuity. It is made available under a CC-BY-NC-ND 4.0 International license.

2.5. Regional analysis

Initially, we analyzed regional ReHo patterns across various brain regions and task conditions. Averaged ReHo values were computed for each region and task condition by aggregating data from all participants and the respective number of runs (2 for tasks, 4 for resting state). This process generated an 8 by 114 matrix. To assess the similarity of ReHo spatial distributions across different task conditions, we computed Pearson's correlation coefficient, producing an 8 by 8 correlation matrix.

Next, for each region we performed a repeated measure analysis of variance (ANOVA) to examine the effects of task on ReHo values (Henson and Penny, 2007). For each region, the mean ReHo values were concatenated across different task conditions and runs and across all the 100 participants, resulting in an 1,800 vector [*(7 x 2 + 1 x 4) x 100*], which served as the dependent variable. The model included 8 regressors representing the eight tasks and 100 regressors representing individual specific effects. We first defined an F contrast representing statistical differences between any of two task conditions. Next, we define F contrast between each of the task condition compared with the resting-state condition.

2.6. Inter-individual correlation analysis

Inter-individual Spearman's correlation coefficient was calculated between the 114 ROIs, resulting in a 114 x 114 covariance matrix. The matrices from the two runs of a task or four runs of the resting state were averaged. Further, the matrices were averaged across the 100 participants, resulting in one matrix for each task/resting-state condition. We calculated Pearson's correlation coefficients of the lower diagonal of the averaged inter-individual correlation matrices between different task and resting-state conditions to estimate their similarity.

To compare the differences in inter-subject correlations between different task conditions, we adopted an inter-individual psychophysiological interaction (PPI) analysis, which is similar to the regular within participant PPI analysis (Di et al., 2020). The model was constructed on each pair of regions of interest, with one as the independent variable and the other as the dependent variable. For both regions, the mean ReHo values across tasks, runs, and participants were concatenated into 1,800 vectors. Before

bioRxiv preprint doi: https://doi.org/10.1101/2024.06.02.597063; this version posted June 3, 2024. The copyright holder for this preprint (which was not certified by peer review) is the author/funder, who has granted bioRxiv a license to display the preprint in perpetuity. It is made available under a CC-BY-NC-ND 4.0 International license.

concatenation, the ReHo values were z transformed for each run to normalize the variances. The model included eight regressors representing the task conditions, eight regressors representing ReHo variations of a region in the eight task conditions, and 100 regressors represent participant specific effects. Please note that this PPI model is an extension to the repeated measure ANOVA model by adding the eight regressors of ReHo values in different task conditions. The regression coefficients of these regressors represent inter-individual correlations between the two regions in a particular condition. Similarly, we defined an F contrast to examine the differences in correlations between any of the two conditions. Further, we also defined F contrasts between each of the task conditions compared with the resting-state condition.

3. Results

3.1. Regional effects of ReHo

Figure S1 depicts the average ReHo maps for the eight task conditions, showing similar spatial distributions of ReHo values across these conditions. In Figure 1A, we further demonstrate the mean ReHo values across 114 ROI for these task conditions. To assess the variance attributed to tasks versus brain regions in these mean ReHo values (Figure 1A), we used a 2-way ANOVA analysis model. Task conditions explained a variance of only 0.0036, whereas regions explained a larger variance of 0.2831. Moreover, the mean ReHo patterns across regions were strongly correlated across different task conditions (Figure 1B), with correlation coefficients ranging from 0.7491 to 0.9740. The lower correlations were primarily observed between the motor task and other task conditions.

bioRxiv preprint doi: https://doi.org/10.1101/2024.06.02.597063; this version posted June 3, 2024. The copyright holder for this preprint (which was not certified by peer review) is the author/funder, who has granted bioRxiv a license to display the preprint in perpetuity. It is made available under a CC-BY-NC-ND 4.0 International license.

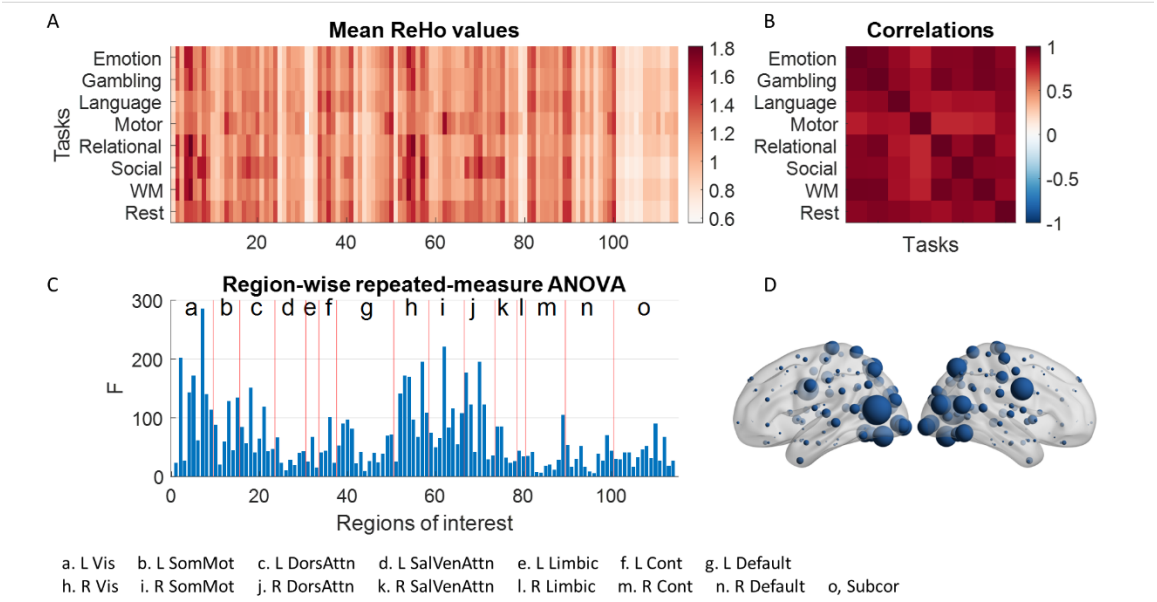


Figure 1 A, mean regional homogeneity (ReHo) for different brain regions of interest and under different task conditions. B, correlations of the mean ReHo values across regions between different task conditions. C, F statistics of a repeated-measure one-way analysis of variance (ANOVA) with task conditions as the within-subject factor for each of the region. The vertical lines in C separate different functional networks shown in the bottom. D, Brain representation of the F values in region-wise repeated-measure ANOVA.

We utilized repeated measure one-way ANOVA for each region, with task conditions as the within-subject factor, to pinpoint regions influenced by task conditions. Figure 1C illustrates the F values for the repeated-measure factor per region, indicating the extent of differences in ReHo among the eight task conditions. Notably, most of the F statistics were statistically significant. However, what's particularly intriguing are the regions with relatively high F values. Figure 1D reveals that these high F value regions were predominantly situated in the posterior visual regions. Additionally, some sensorimotor network and dorsal attention network regions also exhibited elevated F values compared to other brain regions.

The resting-state condition naturally acts as a control condition for the other tasks. Consequently, we compared each task condition to the resting-state condition (refer to Figure 2). The regions displaying

bioRxiv preprint doi: https://doi.org/10.1101/2024.06.02.597063; this version posted June 3, 2024. The copyright holder for this preprint (which was not certified by peer review) is the author/funder, who has granted bioRxiv a license to display the preprint in perpetuity. It is made available under a CC-BY-NC-ND 4.0 International license.

decreased ReHo were primarily within the sensorimotor and dorsal attention networks, notably not the default mode network. Regions exhibiting increased ReHo compared to the resting state varied depending on the tasks. Tasks involving visual stimuli typically led to increased ReHo in visual regions. Additionally, ReHo in certain subcortical regions increased during the gambling task, language task, and notably, the motor task.

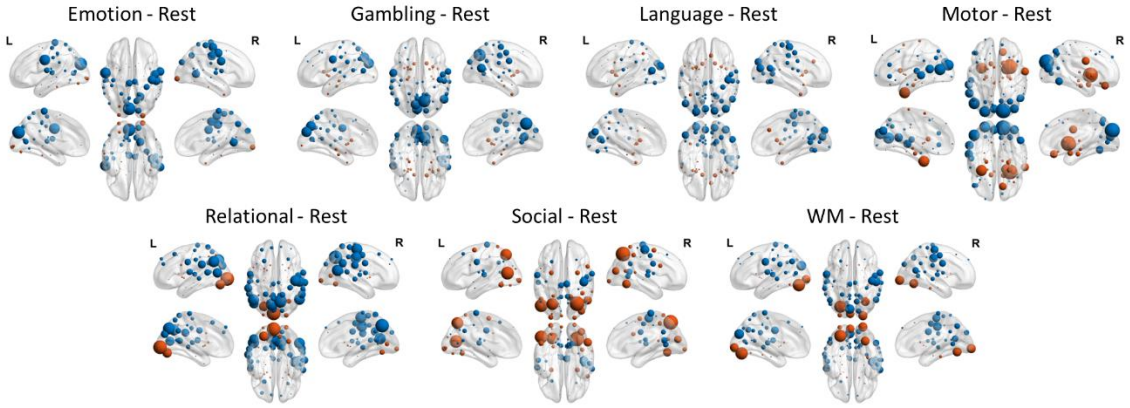


Figure 2 Differences in regional homogeneity (ReHo) between a task condition and the resting-state condition. Red indicates task greater than rest, and blue indicate rest greater than task. The size of the nodes represents F statistics of the specific contrast without thresholding.

3.2. Inter-individual correlations

The inter-individual correlation matrices for different task and resting-state runs are depicted in Figure 3. It's evident that these matrices for different task conditions are largely similar. Specifically, within-network connectivity tended to be stronger than between-network connectivity, as seen by the higher values along the diagonal squares. Moreover, there was notable correlation between corresponding networks in the left and right hemispheres. Subcortical regions also displayed strong correlations among themselves, visible in the bottom right corners of the matrices.

To quantify the similarity across task conditions, we computed correlation coefficients between vectorized upper triangular of the matrices for each task. These matrices exhibited high correlations (ranging from 0.7807 to 0.9386). Notably, all seven task conditions showed extremely high correlations

bioRxiv preprint doi: https://doi.org/10.1101/2024.06.02.597063; this version posted June 3, 2024. The copyright holder for this preprint (which was not certified by peer review) is the author/funder, who has granted bioRxiv a license to display the preprint in perpetuity. It is made available under a CC-BY-NC-ND 4.0 International license.

among each other (around 0.9), while the correlation between the resting condition and task conditions was slightly lower (around 0.8).

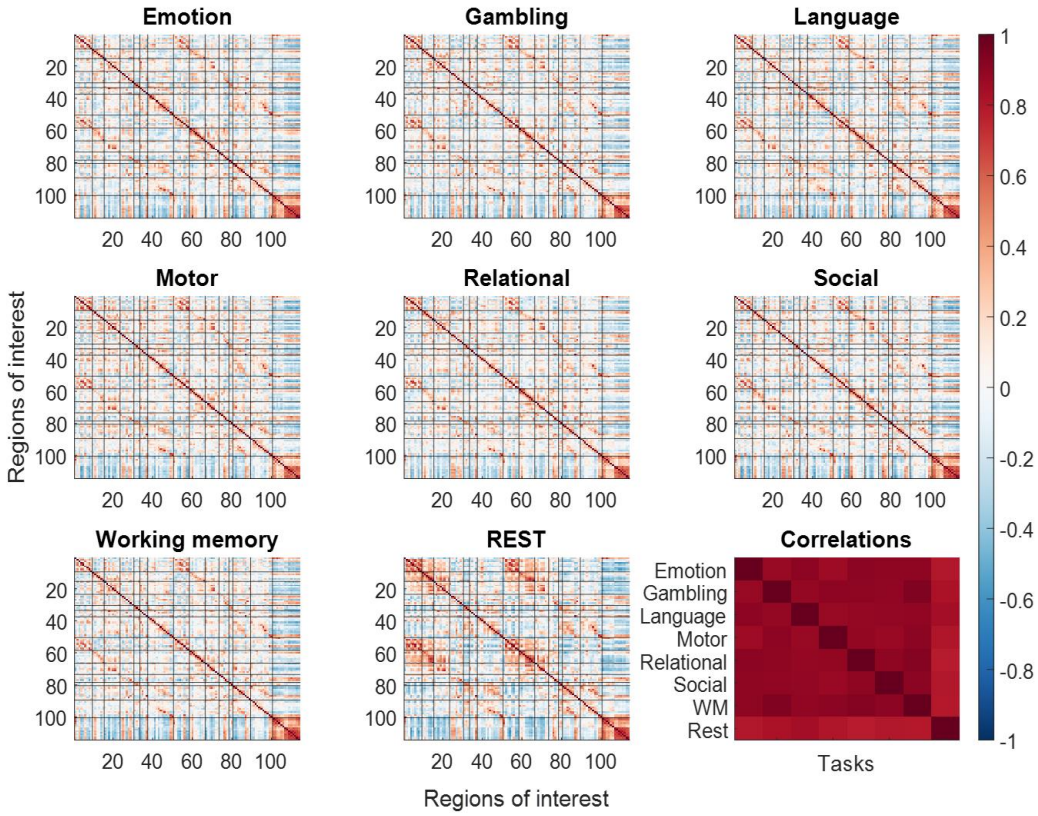


Figure 3 Inter-individual correlation matrices among 114 regions of interest for different task/resting-state conditions. The black lines separate different functional networks. The right most panel in the bottom row shows the correlations of the lower diagonal of the inter-individual correlation matrices among the task and resting-state conditions.

To pinpoint region pairs whose connectivity is influenced by task conditions, we conducted an inter-subject PPI analysis. This involved employing a repeated-measures ANOVA to detect connectivity that showed significant differences across various task conditions. Although the statistical results differed when one region was treated as the dependent variable and the other as the independent variable, they were generally similar. Consequently, we averaged the lower and upper diagonals to create a symmetrical

bioRxiv preprint doi: https://doi.org/10.1101/2024.06.02.597063; this version posted June 3, 2024. The copyright holder for this preprint (which was not certified by peer review) is the author/funder, who has granted bioRxiv a license to display the preprint in perpetuity. It is made available under a CC-BY-NC-ND 4.0 International license.

matrix (refer to Figure 4). The critical F value for $p < 0.001$ was recorded as 3.50. However, no threshold was applied to the matrix to display all task-modulated connectivity effects. The connections displaying modulated connectivity due to tasks were predominantly within the visual network, somatomotor network, the control network, and among these three networks.

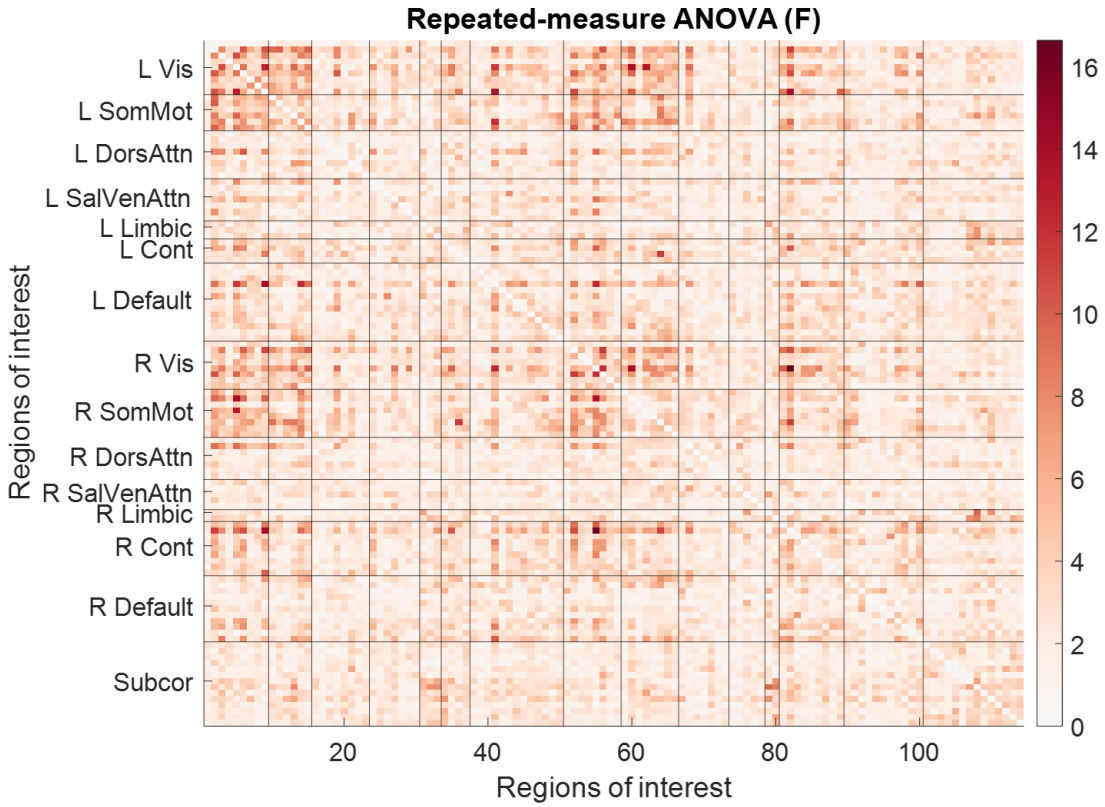


Figure 4 Statistics (F) that reflects the changes of cross-subject connectivity between any pair of tasks (repeated-measure analysis of variance, ANOVA). The black lines separate different functional networks.

We further contrasted the correlation matrices of each task condition with respect to the resting-state condition (Figure 5). It shows that the general pattern of altered covariance in different task conditions with respect to the resting-state were very similar across tasks. In general, reduced correlations were found within the visual network, sensorimotor network, and between the visual and sensorimotor networks. In contrast, increased correlations were found between the control network and the visual or sensorimotor network, and between the sensorimotor and subcortical networks. For a specific task, there

bioRxiv preprint doi: https://doi.org/10.1101/2024.06.02.597063; this version posted June 3, 2024. The copyright holder for this preprint (which was not certified by peer review) is the author/funder, who has granted bioRxiv a license to display the preprint in perpetuity. It is made available under a CC-BY-NC-ND 4.0 International license.

may be unique connectivity modulations, but it is beyond the scope of the current report. To reveal the spatial location of the changes in connectivity for the different tasks, we used BrainNetViewer to show their spatial locations in brain (Figure 6).

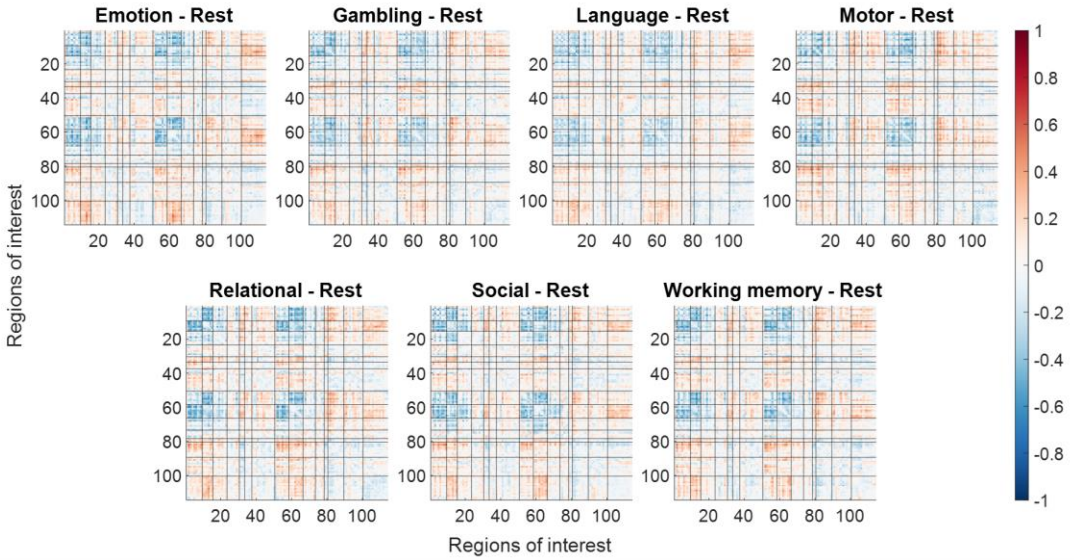


Figure 5 Differences in inter-subject correlations between each task condition with reference to the resting state. The black lines separate different functional networks.

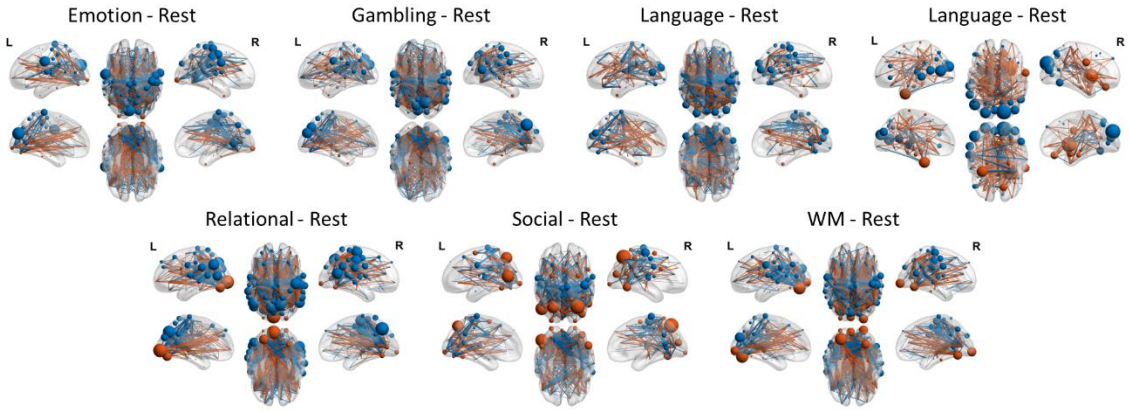


Figure 6 Increased (red) and decreased (blue) cross-subject correlations and regional homogeneity (ReHo) between each task condition compared with the resting condition. The connections were thresholded at $F > 10$, which correspond to a p value of 0.0016. The size of the nodes represents F statistics of the specific contrast without thresholding.

bioRxiv preprint doi: https://doi.org/10.1101/2024.06.02.597063; this version posted June 3, 2024. The copyright holder for this preprint (which was not certified by peer review) is the author/funder, who has granted bioRxiv a license to display the preprint in perpetuity. It is made available under a CC-BY-NC-ND 4.0 International license.

4. Discussion

By using ReHo as a measure of regional brain functions in a temporal scale of minutes, the current analysis showed to what extent ReHo were modulated by different task conditions and how they may affect the estimates of inter-individual correlation measures of brain functional connectivity. The main results can be summarized as follows: First, the changes in ReHo across different task conditions were relatively small compared with the variations across different brain regions, therefore the spatial correlations of ReHo in different task conditions were highly correlated. Second, inter-individual correlations of ReHo among regions of interest in different task conditions were also highly correlated.

The spatial patterns of ReHo were remarkably consistent among all the task conditions, implying that brain structures likely play a significant role in regulating local synchronizations as assessed by ReHo. Notably, numerous cortical regions exhibited elevated ReHo values, contrasting with the generally lower ReHo observed in subcortical regions. This discrepancy may arise from the greater voxel-level homogeneity within cortical areas compared to the heterogeneous nature of subcortical regions, which encompass various subnuclei. These findings present challenges in utilizing the ReHo method to study subcortical brain activity.

ReHo was developed and mainly used on resting-state fMRI data to reflect functions. Regional ReHo values in resting-state were associated task performance in separate testing (Lee and Hsieh, 2017; Tian et al., 2012), and were also correlated with regional task activations in different tasks (Yuan et al., 2013). But to the best of our knowledge, the current study was the first to demonstrate that ReHo can reflect brain functions in different task conditions. Among a wide range of tasks, we pinpointed brain regions that were more likely to be modulated by the task conditions, which include the visual, sensorimotor, and dorsal attention networks. It makes sense because the unimodal regions directly receive input from outside world and generate response, which varied by different task conditions. In contract, the default mode network regions were among the regions that showed the smallest changes in ReHo values in different task conditions. And by directly contrasting each task condition with the resting-state

bioRxiv preprint doi: https://doi.org/10.1101/2024.06.02.597063; this version posted June 3, 2024. The copyright holder for this preprint (which was not certified by peer review) is the author/funder, who has granted bioRxiv a license to display the preprint in perpetuity. It is made available under a CC-BY-NC-ND 4.0 International license.

condition, we further confirmed the regions showed reduced activity in tasks compared with resting-state were mostly sensorimotor, dorsal attention, and visual regions, but not the default mode regions. This result is a little in contrast with PET studies (Shulman et al., 1997), and may reflect the dissociations between glucose metabolism and BOLD oxygenation in the default mode regions (Stiernman et al., 2021).

The regions displaying increased task modulation primarily belong to unimodal brain networks. For instance, the visual networks exhibited increased ReHo values during tasks involving constant visual stimuli, like the emotion task, relational task, social task, and working memory task. Similarly, the auditory region showed elevated ReHo values during the language task, aligning with the auditory nature of the stimuli in this task. Interestingly, the motor regions demonstrated a reduction in ReHo during tasks compared to resting-state conditions. This suggests that task execution involves specific regions within the sensorimotor network, leading to decreased activity in other sensorimotor network regions. Additionally, subcortical regions displayed elevated ReHo values during certain tasks such as the gambling task, language task, motor task, and social task, which is logical given their involvement in motor and reward-related functions. A noteworthy practical implication is that although ReHo values are generally low in subcortical regions, engaging in certain tasks can boost brain activation levels in these regions, thereby enhancing signals within them.

The inter-individual correlations of ReHo were also highly similar across the task conditions, which is consistent with studies of within-individual connectivity (Cole et al., 2014; Di et al., 2020; Krienen et al., 2014). This is also consistent with the high similarity of regional activity, and suggest a common brain network structure may contribute to the highly correlated connectivity structure.

Notable differences in local inter-individual connectivity were also present. The resting state was the most deviate condition and showed relatively lower correlations with all the seven tasks. The connectivity that was modulated by different task conditions can be further categorized into two groups. Firstly, the connectivity within the visual and sensorimotor networks and the connectivity between the two networks typically showed reduced connectivity in any task conditions compared with the resting

bioRxiv preprint doi: https://doi.org/10.1101/2024.06.02.597063; this version posted June 3, 2024. The copyright holder for this preprint (which was not certified by peer review) is the author/funder, who has granted bioRxiv a license to display the preprint in perpetuity. It is made available under a CC-BY-NC-ND 4.0 International license.

state. This is in line with within-individual connectivity changes, where similar connectivity reduction are seen when comparing task conditions with the baseline fixation condition within a task run (Di et al., 2020, 2017b) a separate resting-state run (Cole et al., 2014). Second, the connectivity between the control network and regions from the visual, sensorimotor, and subcortical networks showed increased connectivity in various tasks compared with the resting-state. This is also in line with within-individual comparison between tasks and resting-state (Cole et al., 2014), which in line with the role of the control network as a flexible hub that dynamically connected to other brain regions upon task demands (Cole et al., 2013). Again, a notable absence was the connectivity involving the default mode network, which didn't show much task modulations on connectivity.

Task modulation provides stronger evidence of inter-individual correlations reflecting functional connectivity, contrasting previous mere observations of such correlations. The current findings also carry practical implications for utilizing inter-individual correlation in studying functional connectivity. Specifically, they demonstrate that the overall connectivity pattern remains largely consistent across different task conditions, indicating the feasibility of studying whole-brain functional connectivity in diverse psychological states.

However, subtle yet statistically significant connectivity changes also highlight the importance of considering task design, especially for regions with well-known functions. For instance, if a region of interest is typically activated during a specific task, employing that task may enhance activity and impact correlation estimates with other regions. This consideration is particularly relevant for subcortical regions, where activity is generally weak during resting-state. Additionally, interpretations of results involving sensorimotor regions require attention, as regional activity often decreases during tasks compared to resting-state conditions.

The current analysis has several limitations worth noting. Firstly, it only relied on ReHo to depict regional activity, while alternative methods like the amplitude of low-frequency fluctuations (ALFF) exist (Zang et al., 2007), which could impact inter-individual connectivity patterns (Taylor et al., 2012). However, exploring these different measures falls beyond the scope of the present analysis. Secondly, the

bioRxiv preprint doi: https://doi.org/10.1101/2024.06.02.597063; this version posted June 3, 2024. The copyright holder for this preprint (which was not certified by peer review) is the author/funder, who has granted bioRxiv a license to display the preprint in perpetuity. It is made available under a CC-BY-NC-ND 4.0 International license.

analysis was centered on blood-oxygen-level dependent (BOLD) signals, leaving uncertainties about generalizing these results to molecular imaging. Task-induced signal changes typically remain under 5% in a standard 3T MRI scanner (van der Zwaag et al., 2009; Zandbelt et al., 2008), possibly resulting in limited ReHo alterations. Contrastingly, changes in regional cerebral blood flow and glucose metabolism can lead to significant signal fluctuations. For instance, cerebral blood flow changes measured by arterial spin labeling (ASL) MRI have been reported to range from 10% to 26% during a 2-back task (Kim et al., 2006), while glucose metabolic activity changes vary from 18% to 28% across different tasks and studies (Rischka et al., 2018; Vlassenko et al., 2006). Task-related modulation may be more pronounced in PET imaging due to substantial signal changes, necessitating further systematic investigation.

5. Conclusion

ReHo can be utilized with task fMRI data to capture stable brain functions over minutes. Nevertheless, ReHo values exhibit smaller differences across various task and resting-state scenarios compared with cross-region variations. Inter-individual functional connectivity can be inferred from ReHo values, with whole-brain correlation matrices showing consistency across task and resting-state conditions. Notably, connectivity strength changes were primarily observed between the resting state and other task conditions. While the choice of task may not significantly alter the overall connectivity matrix estimate, it can influence specific connectivity patterns with regions involved in task modulation.

Acknowledgement

The initial idea was developed through discussions with the Molecular Connectivity Working Group (MCWG). The authors would like to thank Dr. Rui Yuan, Marielys Reyes Castillo, and Pushti Shah for their assistance with data curation and image processing. This study was supported by grants from (US) National Institutes of Health for Xin Di (R15MH125332) and Bharat B. Biswal (5R01MH131335).

bioRxiv preprint doi: https://doi.org/10.1101/2024.06.02.597063; this version posted June 3, 2024. The copyright holder for this preprint (which was not certified by peer review) is the author/funder, who has granted bioRxiv a license to display the preprint in perpetuity. It is made available under a CC-BY-NC-ND 4.0 International license.

References:

Adhikari, B.M., Hong, L.E., Zhao, Z., Wang, D.J.J., Thompson, P.M., Jahanshad, N., Zhu, A.H., Holiga, S., Turner, J.A., van Erp, T.G.M., Calhoun, V.D., Hatch, K.S., Bruce, H., Hare, S.M., Chiappelli, J., Goldwaser, E.L., Kvarta, M.D., Ma, Y., Du, X., Nichols, T.E., Shuldiner, A.R., Mitchell, B.D., Dukart, J., Chen, S., Kochunov, P., 2022. Cerebral blood flow and cardiovascular risk effects on resting brain regional homogeneity. NeuroImage 262, 119555. https://doi.org/10.1016/j.neuroimage.2022.119555

Aiello, M., Salvatore, E., Cachia, A., Pappatà, S., Cavaliere, C., Prinster, A., Nicolai, E., Salvatore, M., Baron, J.-C., Quarantelli, M., 2015. Relationship between simultaneously acquired resting-state regional cerebral glucose metabolism and functional MRI: A PET/MR hybrid scanner study. NeuroImage 113, 111–121. https://doi.org/10.1016/j.neuroimage.2015.03.017

Barch, D.M., Burgess, G.C., Harms, M.P., Petersen, S.E., Schlaggar, B.L., Corbetta, M., Glasser, M.F., Curtiss, S., Dixit, S., Feldt, C., Nolan, D., Bryant, E., Hartley, T., Footer, O., Bjork, J.M., Poldrack, R., Smith, S., Johansen-Berg, H., Snyder, A.Z., Van Essen, D.C., 2013. Function in the human connectome: task-fMRI and individual differences in behavior. NeuroImage 80, 169–89. https://doi.org/10.1016/j.neuroimage.2013.05.033

Biswal, B., Yetkin, F.Z., Haughton, V.M., Hyde, J.S., 1995. Functional connectivity in the motor cortex of resting human brain using echo-planar MRI. Magnetic resonance in medicine : official journal of the Society of Magnetic Resonance in Medicine / Society of Magnetic Resonance in Medicine 34, 537–41. https://doi.org/10.1002/mrm.1910340409

Biswal, B.B., Mennes, M., Zuo, X.-N., Gohel, S., Kelly, C., Smith, S.M., Beckmann, C.F., Adelstein, J.S., Buckner, R.L., Colcombe, S., Dogonowski, A.-M., Ernst, M., Fair, D., Hampson, M., Hoptman, M.J., Hyde, J.S., Kiviniemi, V.J., Kötter, R., Li, S.-J., Lin, C.-P., Lowe, M.J., Mackay, C., Madden, D.J., Madsen, K.H., Margulies, D.S., Mayberg, H.S., McMahon, K., Monk, C.S., Mostofsky, S.H., Nagel, B.J., Pekar, J.J., Peltier, S.J., Petersen, S.E., Riedl, V., Rombouts, S.A.R.B., Rypma, B., Schlaggar, B.L., Schmidt, S., Seidler, R.D., Siegle, G.J., Sorg, C., Teng, G.-J., Veijola, J., Villringer, A., Walter, M., Wang, L., Weng, X.-C., Whitfield-Gabrieli, S., Williamson, P., Windischberger, C., Zang, Y.-F., Zhang, H.-Y., Castellanos, F.X., Milham, M.P., 2010. Toward discovery science of human brain function. Proceedings of the National Academy of Sciences of the United States of America 107, 4734–9. https://doi.org/10.1073/pnas.0911855107

Cole, M.W., Bassett, D.S., Power, J.D., Braver, T.S., Petersen, S.E., 2014. Intrinsic and task-evoked network architectures of the human brain. Neuron 83, 238–251. https://doi.org/10.1016/j.neuron.2014.05.014

Cole, M.W., Reynolds, J.R., Power, J.D., Repovs, G., Anticevic, A., Braver, T.S., 2013. Multi-task connectivity reveals flexible hubs for adaptive task control. Nature neuroscience 16, 1348–55. https://doi.org/10.1038/nn.3470

Di, X., Biswal, and Alzheimer's Disease Neu, B.B., 2012. Metabolic Brain Covariant Networks as Revealed by FDG-PET with Reference to Resting-State fMRI Networks. Brain Connectivity 2, 275–283. https://doi.org/10.1089/brain.2012.0086

Di, X., Biswal, B.B., 2019. Toward Task Connectomics: Examining Whole-Brain Task Modulated Connectivity in Different Task Domains. Cereb Cortex 29, 1572–1583. https://doi.org/10.1093/cercor/bhy055

Di, X., Gohel, S., Thielcke, A., Wehrl, H.F., Biswal, B.B., Alzheimer's Disease Neuroimaging Initiative, 2017a. Do all roads lead to Rome? A comparison of brain networks derived from inter-subject volumetric and metabolic covariance and moment-to-moment hemodynamic correlations in old individuals. Brain structure & function 222, 3833–3845. https://doi.org/10.1007/s00429-017-1438-7

bioRxiv preprint doi: https://doi.org/10.1101/2024.06.02.597063; this version posted June 3, 2024. The copyright holder for this preprint (which was not certified by peer review) is the author/funder, who has granted bioRxiv a license to display the preprint in perpetuity. It is made available under a CC-BY-NC-ND 4.0 International license.

Di, X., Reynolds, R.C., Biswal, B.B., 2017b. Imperfect (de)convolution may introduce spurious psychophysiological interactions and how to avoid it. Human brain mapping 38, 1723–1740. https://doi.org/10.1002/hbm.23413

Di, X., Zhang, Z., Biswal, B.B., 2020. Understanding psychophysiological interaction and its relations to beta series correlation. Brain Imaging and Behavior. https://doi.org/10.1007/s11682-020-00304-8

Fang, X.T., Toyonaga, T., Hillmer, A.T., Matuskey, D., Holmes, S.E., Radhakrishnan, R., Mecca, A.P., van Dyck, C.H., D'Souza, D.C., Esterlis, I., Worhunsky, P.D., Carson, R.E., 2021. Identifying brain networks in synaptic density PET (11C-UCB-J) with independent component analysis. NeuroImage 237, 118167. https://doi.org/10.1016/j.neuroimage.2021.118167

Fox, M.D., Snyder, A.Z., Vincent, J.L., Corbetta, M., Van Essen, D.C., Raichle, M.E., 2005. The human brain is intrinsically organized into dynamic, anticorrelated functional networks. Proceedings of the National Academy of Sciences of the United States of America 102, 9673–8.

Frackowiak, R.S.J., Jones, T., Lenzi, G.L., Heather, J.D., 1980. Regional cerebral oxygen utilization and blood flow in normal man using oxygen-15 and positron emission tomography. Acta Neurologica Scandinavica 62, 336–344. https://doi.org/10.1111/j.1600-0404.1980.tb03046.x

Friston, K.J., 2011. Functional and effective connectivity: a review. Brain connectivity 1, 13–36. https://doi.org/10.1089/brain.2011.0008

Friston, K.J., 1994. Functional and effective connectivity in neuroimaging: A synthesis. Human Brain Mapping 2, 56–78. https://doi.org/10.1002/hbm.460020107

Henson, R., Penny, W., 2007. Analysis of variance, in: Statistical Parametric Mapping: The Analysis of Functional Brain Images. Academic Press, London, pp. 193–210.

Horwitz, B., Duara, R., Rapoport, S.I., 1984. Intercorrelations of Glucose Metabolic Rates Between Brain Regions: Application to Healthy Males in a State of Reduced Sensory Input. Journal of Cerebral Blood Flow & Metabolism 4, 484–499. https://doi.org/10.1038/jcbfm.1984.73

Kim, J., Whyte, J., Wang, J., Rao, H., Tang, K.Z., Detre, J.A., 2006. Continuous ASL perfusion fMRI investigation of higher cognition. Neuroimage 31, 376–385. https://doi.org/10.1016/j.neuroimage.2005.11.035

Krienen, F.M., Yeo, B.T.T., Buckner, R.L., 2014. Reconfigurable task-dependent functional coupling modes cluster around a core functional architecture. Philosophical transactions of the Royal Society of London. Series B, Biological sciences 369, 20130526-. https://doi.org/10.1098/rstb.2013.0526

Lee, H.-H., Hsieh, S., 2017. Resting-State fMRI Associated with Stop-Signal Task Performance in Healthy Middle-Aged and Elderly People. Frontiers in Psychology 8.

Li, Z., Zhu, Y., Childress, A.R., Detre, J.A., Wang, Z., 2012. Relations between BOLD fMRI-Derived Resting Brain Activity and Cerebral Blood Flow. PLOS ONE 7, e44556. https://doi.org/10.1371/journal.pone.0044556

Lizarraga, A., Ripp, I., Sala, A., Shi, K., Düring, M., Koch, K., Yakushev, I., 2023. Similarity between structural and proxy estimates of brain connectivity. J Cereb Blood Flow Metab 0271678X231204769. https://doi.org/10.1177/0271678X231204769

Metter, E.J., Riege, W.H., Kuhl, D.E., Phelps, M.E., 1984. Cerebral Metabolic Relationships for Selected Brain Regions in Healthy Adults. Journal of Cerebral Blood Flow & Metabolism 4, 1–7. https://doi.org/10.1038/jcbfm.1984.1

Phelps, M.E., Huang, S.C., Hoffman, E.J., Selin, C., Sokoloff, L., Kuhl, D.E., 1979. Tomographic measurement of local cerebral glucose metabolic rate in humans with (F-18)2-fluoro-2-deoxy-D-glucose: Validation of method. Annals of Neurology 6, 371–388. https://doi.org/10.1002/ana.410060502

Rischka, L., Gryglewski, G., Pfaff, S., Vanicek, T., Hienert, M., Klöbl, M., Hartenbach, M., Haug, A., Wadsak, W., Mitterhauser, M., Hacker, M., Kasper, S., Lanzenberger, R., Hahn, A., 2018. Reduced task durations in functional PET imaging with [18F]FDG approaching that of functional MRI. NeuroImage 181, 323–330. https://doi.org/10.1016/j.neuroimage.2018.06.079

bioRxiv preprint doi: https://doi.org/10.1101/2024.06.02.597063; this version posted June 3, 2024. The copyright holder for this preprint (which was not certified by peer review) is the author/funder, who has granted bioRxiv a license to display the preprint in perpetuity. It is made available under a CC-BY-NC-ND 4.0 International license.

Sala, A., Lizarraga, A., Caminiti, S.P., Calhoun, V.D., Eickhoff, S.B., Habeck, C., Jamadar, S.D., Perani, D., Pereira, J.B., Veronese, M., Yakushev, I., 2023. Brain connectomics: time for a molecular imaging perspective? Trends in Cognitive Sciences 27, 353–366. https://doi.org/10.1016/j.tics.2022.11.015

Schaefer, A., Kong, R., Gordon, E.M., Laumann, T.O., Zuo, X.-N., Holmes, A.J., Eickhoff, S.B., Yeo, B.T.T., 2018. Local-Global Parcellation of the Human Cerebral Cortex from Intrinsic Functional Connectivity MRI. Cerebral cortex (New York, N.Y. : 1991) 28, 3095–3114. https://doi.org/10.1093/cercor/bhx179

Shulman, G.L., Fiez, J.A., Corbetta, M., Buckner, R.L., Miezin, F.M., Raichle, M.E., Petersen, S.E., 1997. Common Blood Flow Changes across Visual Tasks: II. Decreases in Cerebral Cortex. Journal of Cognitive Neuroscience 9, 648–663. https://doi.org/10.1162/jocn.1997.9.5.648

Smith, S.M., Beckmann, C.F., Andersson, J., Auerbach, E.J., Bijsterbosch, J., Douaud, G., Duff, E., Feinberg, D.A., Griffanti, L., Harms, M.P., Kelly, M., Laumann, T., Miller, K.L., Moeller, S., Petersen, S., Power, J., Salimi-Khorshidi, G., Snyder, A.Z., Vu, A.T., Woolrich, M.W., Xu, J., Yacoub, E., Uğurbil, K., Van Essen, D.C., Glasser, M.F., 2013. Resting-state fMRI in the Human Connectome Project. NeuroImage, Mapping the Connectome 80, 144–168. https://doi.org/10.1016/j.neuroimage.2013.05.039

Song, X.-W., Dong, Z.-Y., Long, X.-Y., Li, S.-F., Zuo, X.-N., Zhu, C.-Z., He, Y., Yan, C.-G., Zang, Y.-F., 2011. REST: a toolkit for resting-state functional magnetic resonance imaging data processing. PloS one 6, e25031. https://doi.org/10.1371/journal.pone.0025031

Stiernman, L.J., Grill, F., Hahn, A., Rischka, L., Lanzenberger, R., Panes Lundmark, V., Riklund, K., Axelsson, J., Rieckmann, A., 2021. Dissociations between glucose metabolism and blood oxygenation in the human default mode network revealed by simultaneous PET-fMRI. Proceedings of the National Academy of Sciences 118, e2021913118. https://doi.org/10.1073/pnas.2021913118

Taylor, P.A., Gohel, S., Di, X., Walter, M., Biswal, B.B., 2012. Functional covariance networks: obtaining resting-state networks from intersubject variability. Brain connectivity 2, 203–17. https://doi.org/10.1089/brain.2012.0095

Tian, L., Ren, J., Zang, Y., 2012. Regional homogeneity of resting state fMRI signals predicts Stop signal task performance. NeuroImage 60, 539–544. https://doi.org/10.1016/j.neuroimage.2011.11.098

Tzourio-Mazoyer, N., Landeau, B., Papathanassiou, D., Crivello, F., Etard, O., Delcroix, N., Mazoyer, B., Joliot, M., 2002. Automated anatomical labeling of activations in SPM using a macroscopic anatomical parcellation of the MNI MRI single-subject brain. NeuroImage 15, 273–89. https://doi.org/10.1006/nimg.2001.0978

van der Zwaag, W., Francis, S., Head, K., Peters, A., Gowland, P., Morris, P., Bowtell, R., 2009. fMRI at 1.5, 3 and 7 T: Characterising BOLD signal changes. NeuroImage 47, 1425–1434. https://doi.org/10.1016/j.neuroimage.2009.05.015

Vlassenko, A.G., Rundle, M.M., Mintun, M.A., 2006. Human brain glucose metabolism may evolve during activation: Findings from a modified FDG PET paradigm. NeuroImage 33, 1036–1041. https://doi.org/10.1016/j.neuroimage.2006.06.065

Wang, J., Sun, H., Cui, B., Yang, H., Shan, Y., Dong, C., Zang, Y., Lu, J., 2021. The Relationship Among Glucose Metabolism, Cerebral Blood Flow, and Functional Activity: a Hybrid PET/fMRI Study. Mol Neurobiol 58, 2862–2873. https://doi.org/10.1007/s12035-021-02305-0

Xia, M., Wang, J., He, Y., 2013. BrainNet Viewer: a network visualization tool for human brain connectomics. PloS one 8, e68910. https://doi.org/10.1371/journal.pone.0068910

Yuan, R., Di, X., Kim, E.H., Barik, S., Rypma, B., Biswal, B.B., 2013. Regional homogeneity of resting-state fMRI contributes to both neurovascular and task activation variations. Magnetic resonance imaging 31, 1492–500. https://doi.org/10.1016/j.mri.2013.07.005

Zandbelt, B.B., Gladwin, T.E., Raemaekers, M., van Buuren, M., Neggers, S.F., Kahn, R.S., Ramsey, N.F., Vink, M., 2008. Within-subject variation in BOLD-fMRI signal changes across repeated

bioRxiv preprint doi: https://doi.org/10.1101/2024.06.02.597063; this version posted June 3, 2024. The copyright holder for this preprint (which was not certified by peer review) is the author/funder, who has granted bioRxiv a license to display the preprint in perpetuity. It is made available under a CC-BY-NC-ND 4.0 International license.

measurements: Quantification and implications for sample size. NeuroImage 42, 196–206. https://doi.org/10.1016/j.neuroimage.2008.04.183

Zang, Y., Jiang, T., Lu, Y., He, Y., Tian, L., 2004. Regional homogeneity approach to fMRI data analysis. NeuroImage 22, 394–400. https://doi.org/10.1016/j.neuroimage.2003.12.030

Zang, Y.-F., He, Y., Zhu, C.-Z., Cao, Q.-J., Sui, M.-Q., Liang, M., Tian, L.-X., Jiang, T.-Z., Wang, Y.-F., 2007. Altered baseline brain activity in children with ADHD revealed by resting-state functional MRI. Brain & development 29, 83–91. https://doi.org/10.1016/j.braindev.2006.07.002

bioRxiv preprint doi: https://doi.org/10.1101/2024.06.02.597063; this version posted June 3, 2024. The copyright holder for this preprint (which was not certified by peer review) is the author/funder, who has granted bioRxiv a license to display the preprint in perpetuity. It is made available under a CC-BY-NC-ND 4.0 International license.

Supplementary materials

Supplementary Figure S1 Averaged regional homogeneity (ReHo) images for each task across individuals and runs.

